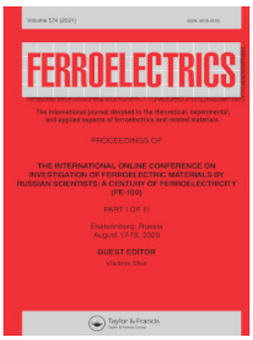

Ferroelectrics

ISSN: (Print) (Online) Journal homepage: https://www.tandfonline.com/loi/gfer20

Pyroelectric drift of integrated-optical $LiNbO_3$ modulators

S. M. Kostritskii, Yu. N. Korkishko, V. A. Fedorov & A. V. Yatsenko

To cite this article: S. M. Kostritskii, Yu. N. Korkishko, V. A. Fedorov & A. V. Yatsenko (2021) Pyroelectric drift of integrated-optical $LiNbO_3$ modulators, Ferroelectrics, 574:1, 170-178, DOI: 10.1080/00150193.2021.1888062

To link to this article: https://doi.org/10.1080/00150193.2021.1888062

Published online: 30 Apr 2021.

FERROELECTRICS
2021, VOL. 574, 170–178
https://doi.org/10.1080/00150193.2021.1888062

Taylor & Francis
Taylor & Francis Group

Pyroelectric drift of integrated-optical $LiNbO_3$ modulators

S. M. Kostritskii[a], Yu. N. Korkishko[a], V. A. Fedorov[a], and A. V. Yatsenko[b]

[a]Optolink Ltd, Zelenograd, Moscow, Russia; [b]Physics and Technology Institute, Simferopol, Russia

ABSTRACT

The pyroelectric response has been studied for electro-optic modulators utilizing *X*-cut $LiNbO_3$ integrated-optical chips. Since this response induces the modulator drift that appears only at fast change of a chip temperature, it causes the temperature and temporal instabilities of integrated-optical devices utilizing these chips. This drift was significantly reduced with the aid of extra electrodes providing the significant shielding of the pyroelectric field.

ARTICLE HISTORY
Received 17 August 2020
Accepted 30 December 2020

KEYWORDS
Lithium niobate; integrated optics; pyroelectric effect; electro-optic modulator

1. Introduction

One of the practical difficulties in the application of $LiNbO_3$ devices is the pyroelectric sensitivity of $LiNbO_3$, which resulted in the appearance of large internal fields within the integrated optical chip (IOC) when subjected to temperature changes or gradients across the device utilizing such an IOC [1–4]. This is because a change in temperature causes a change in the spontaneous polarization due to the ferroelectric properties of $LiNbO_3$. This results in an imbalance of charge at the $\pm Z$ faces of the lateral edges of IOC, so that an electric field is generated in the Z direction perpendicularly to the waveguide paths on $-X$ face of IOC. Due to the very high resistivity of $LiNbO_3$, the screening charges take a long time to travel through the electro-optical crystal and neutralize the bound charges at the polar faces. This imbalance of charge impedes or lessens the effect of the electrical fields from the electrodes on the waveguide paths, thus decreasing the effectiveness of control in modulating optical signals [1, 2, 4]. Thus, the effect of the electric field and the consistency of the effect of the electric field over time (i.e. temporal stability) applied to the waveguide paths should be greatly affected by pyroelectric effect, if there is some temperature variation over time. The amount of electric field from the electrodes that is affected by the pyroelectrically-induced charge imbalance in the $LiNbO_3$ IOC is referred to as the pyroelectric drift of the modulator.

The IOC fabricated on lithium niobate ($LiNbO_3$) *X*-cut wafers (Fig. 1), using conventional techniques to form large numbers of the channel proton-exchanged waveguides and coplanar electrodes, is the main part of the multifunction integrated-optical circuit (MIOC) [1–3]. The MIOC consisting of a beam splitter/combiner, PM-fiber-pigtailed light polarizer and two electro-optical phase modulators (Fig. 2) represents a key part of fiber optical gyroscope (FOG) [2, 3, 5]. It has been established that the MIOC's half-wave voltage depends on the temperature variation [5]. This dependence has been

CONTACT S. M. Kostritskii skostritskii@optolink.ru

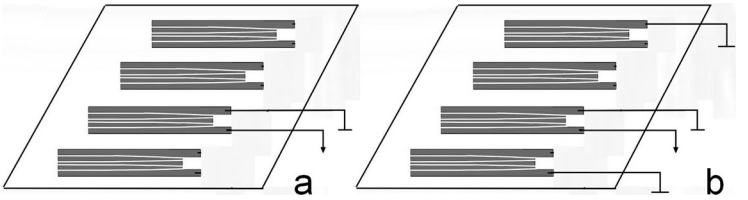

Figure 1. A schematic sketch of an IOC preform. This preform is used for fabrication of four IOCs. Black elements show four groups of the Au/Cr-electrodes deposited on *–X* surface. Each IOC contains one group of the modulator electrodes. Arrows show connection of one modulator electrode with an input port of electrometric amplifier. Two variants of electrical connection are shown: (a) extra electrodes (regular modulator electrodes of other IOCs) are not grounded; (b) these extra electrodes are grounded.

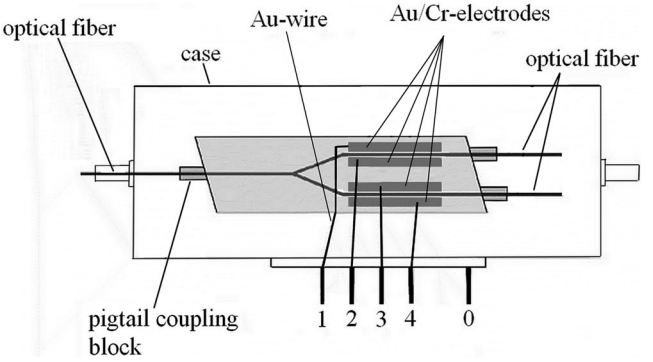

Figure 2. The intrinsic structure of MIOC containing inside a single IOC (shown by light gray color): pins 1-4 are connected by Au-wires with the Au/Cr-electrodes of the electro-optic modulator on a single $LiNbO_3$ chip, Au/Cr-electrodes are shown by dark gray color, the proton-exchanged channel waveguides and *Y*-splitter are shown by black lines within the single IOC, input and output waveguides of IOC are pigtailed with optical fibers.

regarded as an important source of the MIOC modulation phase error, which has significant influence on a temperature stability of the MIOC. The pyroelectric effect is considered by us to be a dominating source of the thermal instability of IOC and hence, MIOC. The detailed experimental study of this effect, allowing for its suppression, has been performed in our paper.

2. Experimental

The experimental study of the pyroelectric response has been made for an unpigtailed IOCs fabricated on *X*-cut $LiNbO_3$ plate. Each IOC contains the coplanar Au/Cr electrodes consisting of the two electro-optic phase modulators of MIOC on main *–X* surface (Fig. 1). The IOCs studied were subjected to the additional hard cleaning (warm dimethylformamide and deionized water) and drying (dry dustless air flow and propanol steam) treatments. Note that IOC preforms studied have extra electrodes in addition to the electrodes of an electro-optic modulator used in MIOC: the several Au-Cr electrodes were deposited on *–X* surface of IOC preform and some of these extra electrodes were grounded with Au-wire (Fig. 1b). Also, the pyroelectric response has been studied for

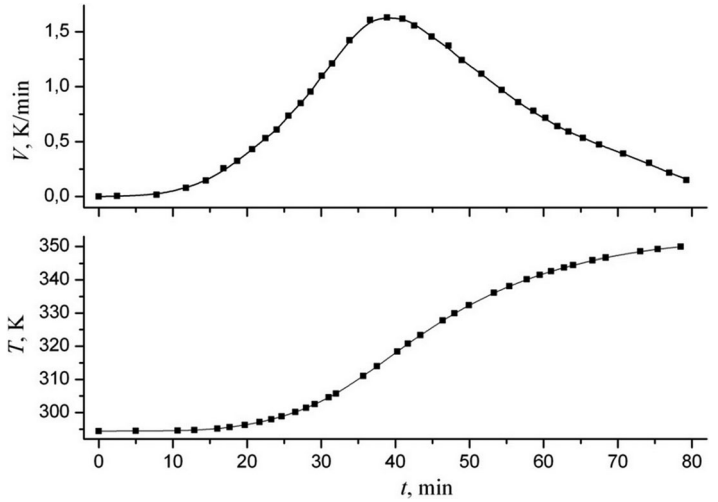

Figure 3. Scanning rate $V = dT/dt$ (upper part) and temperature T (low part) as functions of the scanning time t during heating of the IOC. The rate V of temperature change was gradually varied from 0 to 1.6 K/min, at $\Delta T = 55$ K.

the hermetically-sealed fiber-pigtailed $LiNbO_3$ MIOC used in FOG [3, 5]. The schematic sketch of the MIOC is given in Fig. 2.

The pyroelectric response was measured by the method described in the previous papers [3, 6], i.e. the pyroelectric voltage U was directly recorded while changing the temperature T of the sample in the range from 295 to 350 K. The range of temperature scanning rate $V = dT/dt$ covered the interval from ≤ 0.1 to 1.6 K/min (Fig. 3). A load (measuring) resistor R was wired in parallel to the electrometric amplifier input, and U appeared on MIOC pins (or IOC electrodes) was amplified by factor of 5 and recorded with a H307/2 two-coordinate potentiometer (ZIP-Kuban Ltd, Russia), connected to the output of amplifier, whilst a stable zero position of the signal is carefully maintained. The signals that are superimposed by higher frequency noise or other interference can be smoothed using a low pass filter with selected time constants ($1 \div 3$ s). Assuming that for appropriate evaluation of U the amplifier load resistance R should be much smaller than the crystal resistance, the measurements were performed at $R = 1.06$ GΩ. The pyroelectric response after amplification was measured as voltage drop at this resistor. The signals that are superimposed by higher frequency noise or other interference can be smoothed using a low pass filter with selected time constants ($1 \div 3$ s). Besides, the measurements with high temporal resolution (about 1 μs) were performed with an AKIP 72205 A digital oscilloscope (AKIP Ltd, Russia).

The optical parameters of MIOC were measured by coupling depolarized light into the waveguides with the aid of a single mode fiber. A fiber Lyot depolarizer utilizing polarization-maintaining fiber was used to decrease strongly the degree of residual polarization of a superluminescent diode radiation (central wavelength is ~1540 nm) and, hence, minimize a polarization-dependent error in measurement results. To determine insertion losses and splitting ratio, we used a fiber-to-fiber coupling set-up [7]. A RIFOCS 575 L optical power meter (RIFOCS Corp., USA) was used as photodetector. No noticeable changes of insertion losses and splitting ratio were observed during

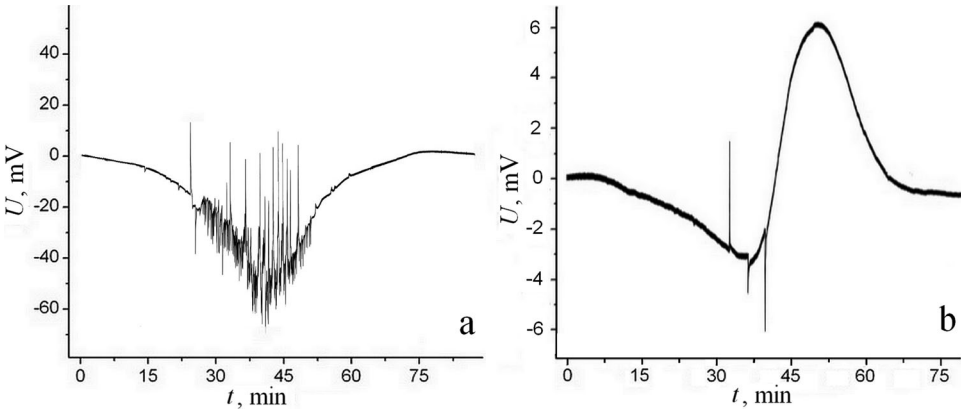

Figure 4. Pyroelectric voltage U measured in the IOC preform (Fig. 1) as a function of scanning time t during heat-up: (a) the electrometric amplifier connected with one modulator electrode, when the extra electrodes on $-X$ face of the IOC preform were not grounded (Fig. 1a); (b) the amplifier connected with one modulator electrode, when the two extra electrodes on $-X$ face of the IOC preform were grounded (Fig. 1b). The load resistance R of the electrometric amplifier is 1.06 GΩ.

temperature changes within the entire range studied by us. It means, that in contrast to the previously reported findings [1, 2, 8], the pyroelectrically-induced hysteresis in the transmitted power of the MIOC caused by the temporal variation of an efficiency of the waveguides in the IOC to propagate light was not observed in our experiments. This peculiarity may be caused by the smaller values of temperature scanning rate in our recent and the previous [7] experiments compared to those reported in Ref. [8].

3. Experimental results and discussion

Application of the coplanar electrodes deposited on a main X-cut face of IOC gives a unique possibility for detailed study of the dielectric [9] and pyroelectric [3] properties of $LiNbO_3$ chips. For example, the slowly changed electric signal with sharp electric pulses is observed in an electrometric amplifier output signal during temperature changes, if some of the modulator electrodes is connected to the amplifier input (Fig. 4). The slowly changed signal is related to the voltage U appearing on the modulator electrodes of IOC and it is found to be monotonously increasing with the temperature scanning rate V. According to the Refs. [1–4], it has been assigned by us to the pyroelectric response of the IOC. According to our data mentioned above, the magnitude of this pyroelectric voltage is not sufficient to induce any marked change of the propagation optical losses for channel waveguide of IOC (extreme case is so-called "shutdown" of channel waveguide [8]). By the way, these voltage values are sufficient to induce the temporal variation of driving voltage (the voltage responsible for the optical modulation) on the IOC and, hence, a marked MIOC phase error should appear. At the same time, the voltage distortion on the modulator in response to the temperature variation is directly related to the pyroelectric voltage U measured (Fig. 4).

Sharp pulses in the electrometer output are related to electric discharges between the lateral $\pm Z$ edges of IOC and between electrodes within an inter-electrode gap. These numerous electrical discharges are detected by electrometer connected to any IOC

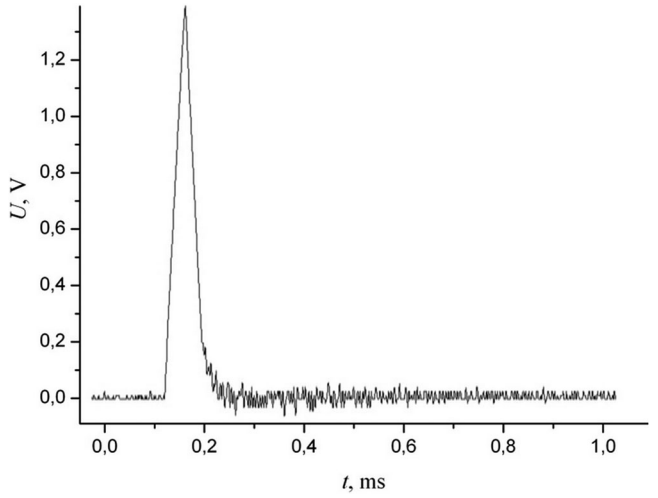

Figure 5. Single pulse of the pyroelectric voltage U measured with the digital oscilloscope without any filtration. This pulse has amplitude of 10 mV during measurement with the electrometric amplifier having the low pass filter (Fig. 4).

electrode (Fig. 4a). They are established to be the other specific feature of the IOC pyroelectric response in addition to the slowly changed voltage U. The data shown in Fig. 4 were obtained with the low-pass filter. Hence, a pulse amplitude is limited by transmission band of the low-pass filter (1 Hz) and also by the response speed of a recording system of our electrometer set-up. However, the real amplitude of these pulses is much larger than that shown in Fig. 4. For example, our measurements with the aid of the digital oscilloscope without using a low pass filter show that the real amplitude of the short ($\approx 0.08 \div 0.11$ ms) pulses is about several Volts that are two orders of magnitude larger than those recorded by the electrometer (Fig. 5). Analysis of the digital oscilloscope data on shape of these short pulses allows evaluating the total electric charge ΔQ_p transferred through the IOC surface with all the pulses (electric discharges):

$$\Delta Q_p = < F > \sum_{i=1}^{N} h_i \tag{1}$$

where F is proportionality parameter and $F = \delta Q_p/h$, δQ_p is electric charge transferred through the IOC surface during a certain pulse studied, h is amplitude for this pulse (e.g., $h = 1.4$ V for the pulse shown in Fig. 5), F is ranged from 42.8 to 53.3 pC/V, $<F> = 48.4$ pC/V is an average value of F for all pulses detected in a single temperature scan, h_i is amplitude of i-th pulse, N is a total quantity of pulses in this temperature scan.

Evaluation from our experimental data with Eq. (1) gives that ΔQ_p is about 12 nC in the cases shown here (Figs. 4a and 5). Note, that ΔQ_p has the quite different values for other experiments, as ΔQ_p depends on cleaning degree of IOC faces and the rate V of a temperature change.

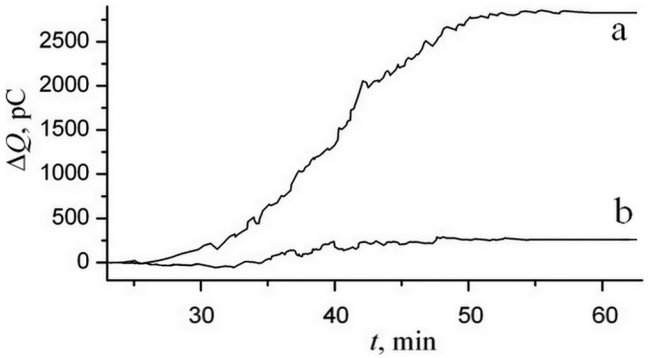

Figure 6. Pyroelectric response of the MIOC (Fig. 2). The total electric charge ΔQ appearing on a modulator electrode of the IOC was evaluated by Eqs. (1–3) from measurement of $U(t)$ with the electrometric amplifier: (a) amplifier input was connected to the pin #1 of MIOC when the two pins #2 and #3 were grounded; (b) amplifier input was connected to the pin #2 of MIOC when the two pins #1 and #4 were grounded.

On the other hand, the electric charge ΔQ_{sc} transferred through the amplifier load resistor during measurement of the slowly changed signal $U(t)$ can be calculated by:

$$\Delta Q_{sc} = \int I(t)\mathrm{d}t,\ I(t)\ = U(t)/(K \times R) \tag{2}$$

where K is an amplification factor ($K = 5$ for our all experiments), R is an amplifier load resistance, $I(t)$ is a pyroelectric current evaluated from our experimental data on $U(t)$ (Fig. 4a).

Calculation by Eq. (2) gives the value $\Delta Q_{sc} = 125$ nC for the case shown in Fig. 4a. Thus, the total electric charge ΔQ generated by IOC can be estimated from our data as:

$$\Delta Q = \Delta Q_p + \Delta Q_{sc} = \ 137\ \mathrm{nC} \tag{3}$$

It is important to note, that this value coincides practically with the theoretically expected value of the total electric charge ΔQ_T generated by the IOC, as $\Delta Q_T = \gamma \times \Delta T \times S = 148.5$ nC, where $\gamma = 100\ \mu\mathrm{C/m^2K}$ is a pyroelectric coefficient for $LiNbO_3$ [6, 9], $S = 27 \times 10^{-6}\ \mathrm{m^2}$ is the area of a lateral polar face of IOC. The temperature changes within the range from 295 to 350 K, i.e. $\Delta T = 55$ K during this temperature scan, which is shown in Fig. 3.

Of course, such a strong pyroelectric response will present a serious problem for application of the IOCs in various devices, e.g. in MIOCs. The pyroelectric $U(t)$ will induce temporal variations of the driving voltage due to superposition with the externally applied modulating voltage. These variations represent the pyroelectric drift of the modulator. According to the previously reported finding [1, 2], we assume that the effect of the differential charge appearance between modulator electrodes may be reduced by shielding between modulator electrodes and the polar $\pm Z$ faces of IOC. Note that our approach is different from the previously proposed ones, where either the total conductive coating of the lateral polar $\pm Z$ faces was applied [1], or the extra electrodes ("metallic rails" [2]) were positioned very close to input waveguide and Y-junction section of IOC. In fact, such a partial shielding was effectively applied by us with the aid of grounding of extra electrodes deposited on -X surface between polar $\pm Z$ faces and

modulator electrodes (Figs. 1b and 4b), but the input waveguide and *Y*-junction section (see the left part of the IOC shown in Fig. 2) were not shielded. By the way, the IOC generates just the same pyroelectric charges ΔQ as in the first experiment (Fig. 4a), because ΔT and V(t) were constant in our experiments (Figs. 4–7). Note, that this result was obtained with the experimental sample of the IOC preform used for fabrication of four single IOC. However, we propose to apply this approach for suppression of the pyroelectric drift of modulator in the single IOCs that will allow improving thermal stability of the industrial MIOCs.

The pyroelectric response of the IOC with grounded additional electrodes demonstrates the change of sign (Fig. 4b). It may be explained by the fact that the additional electrodes create a gradient in the local surface potential near the electrodes when unscreened pyroelectrically induced surface charges are present [10]. Therefore, we consider a related contribution of the so-called electrostatic component [10] for explanation of the pyroelectric response of IOC. This component is strong in the case of *Z*-cut IOCs [10], and should be much weaker in the case of *X*-cut IOCs [3, 10]. The amplitude and sign of this component were changed when the electrodes were contacted (e.g., grounded) [10]. According to our data, this component becomes noticeable in the case of the grounded additional electrodes, when the "pyroelectric component" (see definition given in Ref. [10]) is strongly suppressed and the two competitive components are observed (Fig. 4b).

To verify efficiency of this approach for the single IOC, we made the following experiments with a standard MIOC (Fig. 2) produced by RPC Optolink [10]. The two external electrodes of the modulator were used for shielding as the both MIOC pins #1 and #4 were grounded. The pyroelectric response was measured by connection of the one MIOC pin #2 or #3 with input of electrometric amplifier circuit, i.e. the pyroelectric voltage was probed with one internal modulator electrode. This measurement demonstrated the strongly reduced pyroelectric response (Fig. 6b) in comparison with the other experiment (Fig. 6a), when the pyroelectric voltage was probed with external modulator electrodes (electrometer input connected with the one MIOC pin #1 or #4) and the two MIOC pins #2 and #3 were grounded simultaneously (Fig. 2). The same effective shielding of the internal probing electrode (pins #2 or #3) was achieved by grounding the other internal electrode and one external electrode (pins #1 or #4) (Fig. 2). At the same time, the comparison of the ΔQ values obtained by us for the IOC perform (Eq. (3)) and for the MIOC (Fig. 6a) demonstrates that the shielding between the probing modulator electrode and only one polar lateral face ($+Z$ or $-Z$) of the IOC provides rather strong suppression of the differential charge appearance. This result is in accordance with our previous data [3] on the significant reduction of the IOC's pyroelectric response at the shielding of the modulator electrode from one polar face with the aid of the extra electrodes. Such a partial shielding provides the significant reduction of the inter-electrode capacitances, giving a marked contribution to reduction of the pyroelectric voltage $U(t)$ [3]. Note that all these electric connection modes of the MIOC are out of practical interest for application in FOG [5, 11], but they demonstrate the principal possibility of the shielding of differential charge arising between the modulator electrodes, using the extra electrodes in the single IOC.

We assume that special metallization should be applied to a small portion of the top –*X* face of the single IOC to form two extra technological electrodes in addition to four modulator electrodes. These short extra technological electrodes must be grounded (or electrically connected) and positioned near the modulator electrodes and close to the two IOC edges, which are perpendicular to *Z* axis direction. The extra electrodes may be arranged in single IOC by the simple modification of photolithography/metallization technology and they will be used to prevent a charge differential from developing between the modulator electrodes, reducing the pyroelectric drift of modulators within IOC and, hence, improving the thermal stability of MIOC. Moreover, some additional improvement of the temperature stability of MIOC would be possible to obtain by some optimization of the extra and modulator electrodes [4, 12, 13]. It will be a subject of our further study.

4. Conclusion

The pyroelectric response in the *X*-cut $LiNbO_3$ chips may reach a significant magnitude at a fast change of temperature; thus, it should induce the modulator drift causing the temperature and temporal instabilities of integrated-optical devices (e.g. MIOC) utilizing these chips. The modulator drift is related to variation of driving voltage (the voltage responsible for the optical modulation) due to a superposition of the externally applied modulating voltage with the time-dependent pyroelectric voltage generated by the IOC. The pyroelectric response and the sequent driving voltage distortion are proportional to the temperature variation rate. The pyroelectric response and drift were significantly reduced with the aid of the extra electrodes providing the significant shielding of the differential charge appearance between the modulator electrodes in the IOCs and MIOCs studied.

References

[1] K. W. Shafer *et al.*, Integrated optics chip with reduced thermal errors due to pyroelectric effects, US Patent, 6044184 (2000).

[2] L. L. Gampp *et al.*, Dual purpose input electrode structure for MIOCs (multi-function integrated optics chips), US Patent, 6128424 (2000).

[3] S. M. Kostritskii *et al.*, Dependence of pyroelectric response on inter-electrode capacitance for integrated-optical circuits utilizing x-cut $LiNbO_3$ chips, *IOP Conf. Ser: Mater. Sci. Eng.* **699**, 012021 (2019). DOI: 10.1088/1757-899X/699/1/012021.

[4] C. H. Bulmer, W. K. Burns, and S. C. Hiser, Pyroelectric effects in $LiNbO_3$ channel waveguide devices, *Appl. Phys. Lett.* **48** (16), 1036 (1986). DOI: 10.1063/1.96640.

[5] R. Bi *et al.*, Temperature modeling of modulation phase error in the integrated optical chip for closed-loop interferometric fiber optic gyroscope, *Opt. Eng.* **58** (06), 1 (2019). DOI: 10.1117/1.OE.58.6.067104.

[6] A. V. Yatsenko *et al.*, Features of the electrical properties of lithium niobate crystals grown from a melt containing K_2O flux, *Phys. Solid State* **61** (7), 1211 (2019)., DOI: 10.1134/S106378341907031X.

[7] S. M. Kostritskii, Photorefractive effect in $LiNbO_3$-based integrated optical circuits at wavelengths of third telecom window, *Appl. Phys. B.* **95** (3), 421 (2009). DOI: 10.1007/s00340-009-3501-4.

[8] R. S. Ponomarev, D. I. Shevtsov, and P. V. Karnaushkin, "Shutdown" of the proton exchanged channel waveguide in the phase modulator under the influence of the pyroelectric effect, *Appl. Sci.* **9** (21), 4585 (2019). 1 DOI: 10.3390/app9214585.

[9] A. V. Yatsenko, and S. M. Kostritskii, Influence of a constant electric field on the dielectric properties of $LiNbO_3$, *Tech. Phys.* **65** (4), 622 (2020). DOI: 10.1134/S1063784220040258.

[10] P. Skeath *et al.*, Novel electrostatic mechanism in the thermal instability of z-cut $LiNbO_3$ interferometers, *Appl. Phys. Lett.* **49** (19), 1221 (1986). DOI: 10.1063/1.97419.

[11] Y. N. Korkishko *et al.*, Interferometric closed-loop fiber-optic gyroscopes, *Proc. SPIE* **8351**, 83513L (2012). DOI: 10.1117/12.966358.

[12] R. A. Becker, Circuit effect in $LiNbO_3$ channel-waveguide modulators, *Opt. Lett.* **10** (8), 417 (1985). DOI: 10.1364/OL.10.000417.

[13] K. Higuma *et al.*, Electrode design to suppress thermal drift in lithium niobate modulators, *Electron. Lett.* **36** (24), 2013 (2000). DOI: 10.1049/el:20001260.